

Combined CL/EBIC/DLTS investigation of a regular dislocation network formed by Si wafer direct bonding

© X. Yu^{*,+,}, O. Vyvenko^{+,°}, M. Kittler^{*,+,}, W. Seifert^{*,+,}, T. Mtchedlidze⁺, T. Arguirov^{*,+,}, M. Reiche[≠]

*IHP,
15236 Frankfurt (Oder), Germany

+ IHP/BTU Joint Lab,
03046 Cottbus, Germany

≠ MPI für Mikrostrukturphysik,
06120 Halle, Germany

° St. Petersburg State University,
198504 St. Petersburg, Russia

(Получена 12 сентября 2006 г. Принята к печати 3 октября 2006 г.)

Electrical levels of the dislocation network in Si and recombination processes via these levels were studied by means of the combination of grain-boundary deep level transient spectroscopy, grain-boundary electron beam induced current (GB-EBIC) and cathodoluminescence (CL). It was found two deep level traps and one shallow trap existed at the interface of bonded interface, which supply the recombination centers for carriers. The total recombination probability based on GB-EBIC data increased with the excitation level monotonically, however, the radiative recombination based on D1–D2 CL data exhibited a maximum at a certain excitation level. By applying an external bias across the bonded interface, the CL signal of D-lines was enhanced dramatically. These results are consistent with our models about two channels of recombination via the trap levels.

PACS: 68.37.Hk, 71.55.Cn, 78.60.Hk

1. Introduction

Si-based light emitters with efficient emission at 1.5 or 1.3 μm are required for on-chip optical interconnection for ultra large scale integrated circuits (ULSI) in the future. Recently, a room-temperature light emitting diode (LED) with efficiency of 0.1% has been fabricated based on the D-lines in the deformed Si [1]. Unfortunately, plastic deformation cannot be immediately used for the industrial device fabrication. A reproducible approach to form a regular dislocation network is silicon wafer direct bonding. Such a dislocation network has been reported to exhibit D-lines cathodoluminescence (CL) [2] and was recently suggested as a promising candidate for the dislocation based LED in our previous paper [3,4]. By proper chosen misorientation, the bonded wafers could emit the light at the desired wavelengths of about 1.5 or 1.3 μm [5]. Moreover, it was found that the D-line CL signal in the *p*-type bonded wafers could be dramatically enhanced when an external bias voltage was applied across the bonded interface [5].

In this paper we will try to find the relationship between the electrical levels and the recombination processes via the states of the dislocation network, which based on the combination of different methods such as capacitance transient spectroscopy of deep levels (GB-DLTS), thermally stimulated capacitance (GB-TSCap), electron beam induced current (GB-EBIC) and CL under applied voltage.

2. Experiment

Two *p*-type Czochralski (CZ) grown (100) Si wafers with a diameter of 150 mm and with the doping concentration of about $10^{15}/\text{cm}^3$ were used for direct wafer bonding.

After standard chemical and deionized water cleaning, the oxide layer on the wafer surface was removed by dipping in hydrofluoric acid (2%). These two wafers were subsequently bonded at room temperature, which twist and tilt angles are 8.2° and 0.2° respectively. The bonded wafers were annealed for 4 h at 1050°C in dry oxygen ambient to improve the bonding strength. Transmission electron microscope (TEM) investigation showed that the distances between adjacent screw (edge) dislocations at the bonded interface were about 2.6 nm (59 nm) [6]. Secondary ion mass spectroscopy (SIMS) analysis revealed that higher concentration oxygen existed at the bonded interface, comparing with that in the Si substrate.

The samples with a size of 2 × 2 mm were cut from the bonded wafers, and treated in diluted HF. Two Ohmic contacts formed on both the front and back surfaces of samples by evaporating gold or by scratching the InGa alloy. The trap behaviour of dislocation networks in the samples were measured by capacitance voltage (C–V), GB-DLTS as well as GB-TSCap. And the recombination behaviour of carriers via these traps was investigated by GB-EBIC and CL. The GB-EBIC/CL measurements were performed on the cross section of the samples at liquid nitrogen temperature.

3. Results and discussion

3.1. CV/GB-DLTS and CL spectra

Fig. 1 showed the C–V characteristics measured at different temperatures between two ohmic contacts across the bonded interface. At low voltages and at sufficiently high temperatures the C–V curves exhibit a double-diode behaviour indicating the presence of a high barrier at

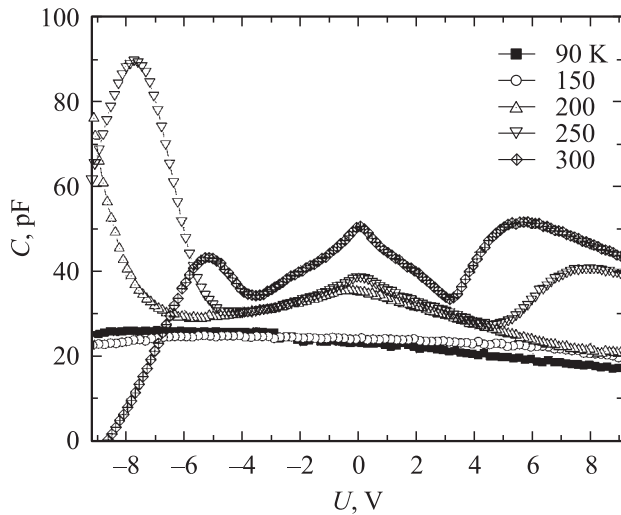


Figure 1. Capacitance–voltage characteristic of *p*-type bonded wafer measured across the boundary at different temperatures.

the bonded interface. In the *C*–*V* curve, some signal peaks are found, which are believed to originate from certain trap response at the frequency of testing voltage (1 MHz) and gives additional contribution to the measured capacitance [7]. The asymmetric distribution of the trap signal peaks at the positive and negative voltages might be related to the resistance difference of prepared Ohmic contacts. From the capacitance change caused by the traps at room temperature, it can be obtained that the total trap density is above 10^{11} cm^{-2} . Furthermore, it is clearly seen that in *C*–*V* curves, the position of some signal peaks shifted to higher voltages with decreasing temperature, which corresponds to the resistance increase of sample and Ohmic contacts at low temperature. The energy level position of this trap responsible for the capacitance peaks was estimated to be about 60–80 mV above the valence band top.

The trap states at the bonded interface were investigated also by GB-DLTS and GB-TSCap techniques based on the fact that application of a bias voltage to the boundary changes the Fermi level position with respect to the electrical levels at the interface and increases the occupancy degree of deep levels with the majority carriers [8]. The results of our GB-DLTS and GB-TSCap measurements (not shown for brevity) revealed three main trap centers with the free enthalpies of the hole ionization of $E_v + 0.3 \text{ eV}$ (DT1), $E_v + 0.4 \text{ eV}$ (DT2) and $E_v + 0.08 \text{ eV}$ (DT3) [5]. The DLTS measurements shows the total trap density is larger than 10^{11} cm^{-2} , which is consistent with the *C*–*V* measurement. The barrier height derived from the capacitance of the structure and from the temperature dependence of the dark current was estimated to be about 0.3–0.4 eV with respect to the Fermi level and in close accordance with T1–T2 level positions.

CL spectra of dislocation networks of our samples at 80 K consisted generally of the superposition of well known dislocation related D1, D2, D3 and D4 lines [1],

a peak around $1.55 \mu\text{m}$ that was previously attributed to the oxygen aggregation at dislocations [9] and a weak line corresponding to band-band transitions. Though the shape of CL spectrum sometimes varied, depending on particular piece of the bonded wafer, the main peak of the luminescence always appeared close to the position of D1 line ($1.5 \mu\text{m}$).

3.2. CL dependence on the excitation level and on the bias voltage

The nature and even a scheme of optical transitions for D1 luminescence is not known precisely at present because it is impossible to find out one-to-one correspondence between the electrical levels registered with capacitance spectroscopy technique and the levels involved in optical transition. Here we tried to supply a new information about the relationship between the electrical levels and the optical transition of dislocation network by using the advantage of the cross sectional GB-EBIC and CL measurements. It is well known that the measurements of GB-EBIC across the boundary reveals the total recombination current of carriers towards the boundary [10]. Depending on the recombination rate immediately at the boundary (RRB) the current can be recombination rate limited or diffusion limited. Whatsoever, the RRB process consists of non-radiative and radiative (D1-CL) recombination components.

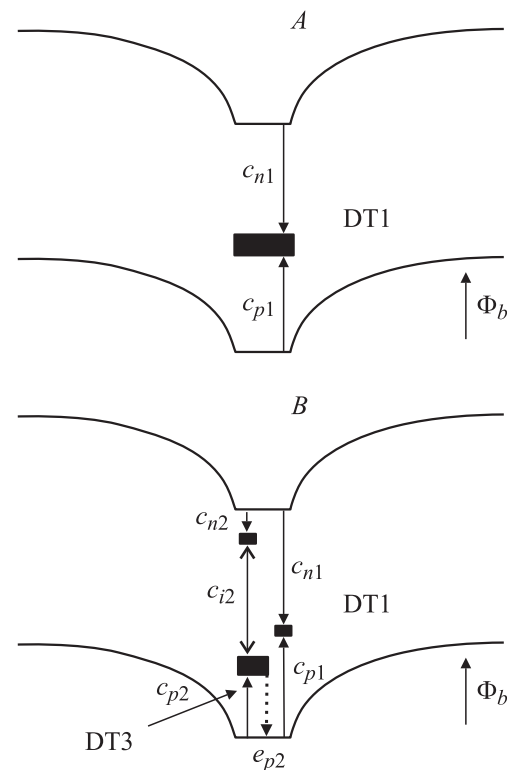


Figure 2. Two models of the recombination via the electrical level at the boundary: *A* — the recombination via one single main deep level; *B* — coupled recombination via two minor shallow levels in the presence of recombination via one single main deep level.

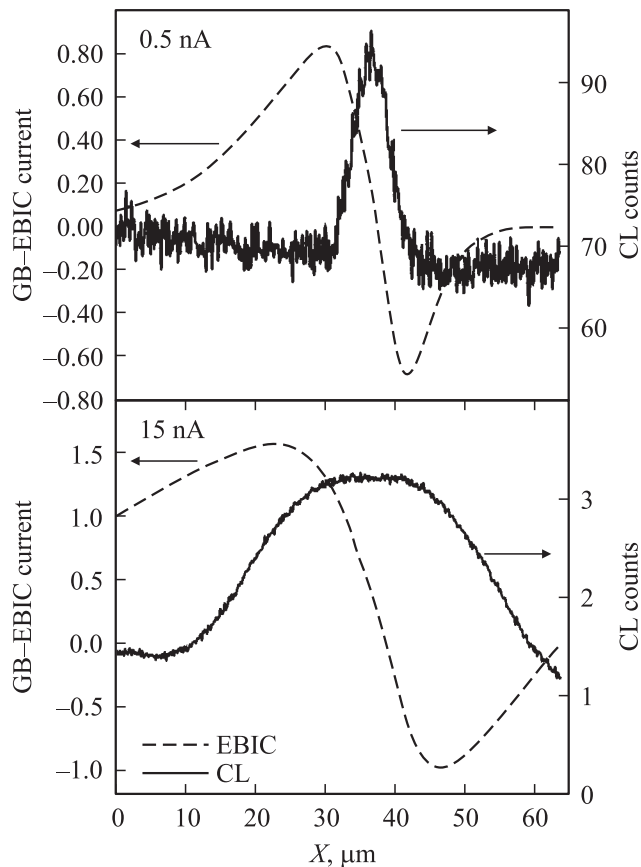


Figure 3. CL (dashed lines) and GB-EBIC (solid lines) profiles across the boundary at two different values of electron beam excitation current. $T = 80$ K.

We calculated the recombination probability (RP) considering two models depicted in Fig. 2. The first model (the model *A* in Fig. 2) assumes that D1 luminescence is a result of the transition between the conduction band and a single level that located 0.3 eV above the valance band top (DT1). The second model (the model *B* in Fig. 2) is that of the coupled radiative recombination occurs via two shallow levels (one of them might be just the level DT3). In both models DT1 is assumed to be the main level at the boundary, and the occupancy of DT1 by the holes defines the barrier height of the bonded interface.

Our calculation showed that the models *A* and *B* had a qualitatively different dependence of the recombination probability on the excitation level as well as on the external bias voltage. The details of these calculations are beyond the scope of this paper and will be published elsewhere. Here we only present a brief description of the calculation results.

The model *A* predicts a monotonic decrease of the recombination probability with increasing the excitation level whereas the model *B* that accounts thermal emission from the DT3 level gives an increase of the RP at low excitation levels, then it reaches a maximum at a intermediate excitation level and, subsequently, RP decreases upon the

excitation increase similar to the model *A*. As a result of applying a variable external bias voltage, the RP keeps practically constant at low voltages and strongly decreasing at higher voltages in the model *A*, but in the model *B*, the RP exhibits a maximum at a certain external bias.

Fig. 3 represents the profiles of GB-EBIC and the panchromatic CL signal across the bonded interface, which were acquired simultaneously during signal scans at a low (Fig. 3, *a*) and a high (Fig. 3, *b*) electron beam currents. At low excitation conditions the shape of the CL profile is Gaussian-like with a width close to distance between the positive and negative peaks of GB-EBIC, i.e. the projected ranges of silicon at the accelerating voltage of 30 kV (compare dashed and solid curves in Fig. 3, *a*). When the excitation current increases by a factor of 30 the distance between the positive and negative peaks of GB-EBIC only doubles whereas the width of CL profile increases by a factor of 6. Additionally, the CL profile becomes flat or one can recognize even a small dip at the center. Based on these observations about the qualitative different changes of GB-EBIC and CL profiles on the excitation level, it is believed that the radiative and total recombinations at the boundary have different mechanisms.

If the efficiency (probability) of the total recombination and the radiative recombinations is simply defined as the ratio of the measured GB-EBIC or CL signals and the electron beam excitation current respectively, after normalizing the efficiency to the value at the lowest excitation current, the variation of total and radiative recombination normalized efficiency with excitation current was shown in Fig. 4. The data for the radiative component were taken from the CL profile center whereas for the total recombination efficiency from the GB-EBIC values at the distances of about $20 \mu\text{m}$ away from the boundary. The

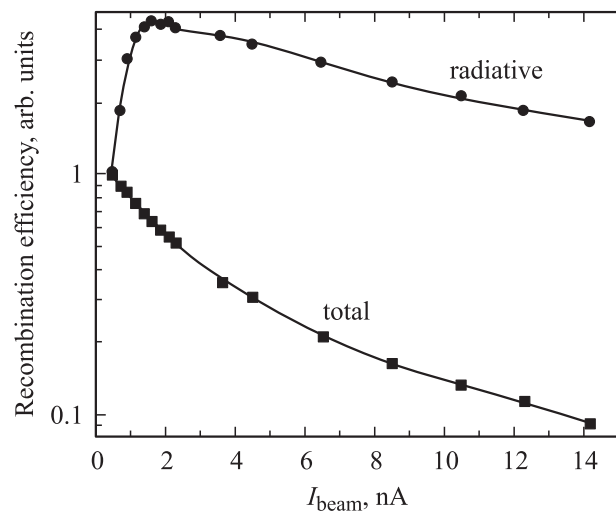


Figure 4. Recombination efficiency (probability) versus electron beam excitation current normalized to the value at the lowest current used. Total recombination: calculated from GB-EBIC data; radiative recombination: calculated from D-line panchromatic CL data.

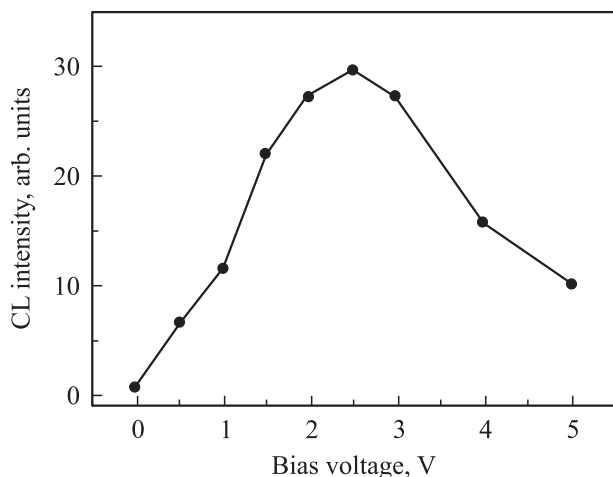


Figure 5. D-line panchromatic CL intensity versus the bias voltage applied across the boundary.

quantitative difference between the total recombination and the radiative component is obvious. The probability of the total recombination decreases monotonically, which corresponds to the recombination via the main deep single level which defines the barrier height at the boundary (model A). The probability of radiative recombination is in agreement with the model B where additional channel of the coupled recombination via two shallow levels was assumed. This conclusion is in concordance with the previously models suggested for D1–D2 luminescence [11,12].

Additional confirmation of this conclusion was the dependence of CL intensity on the external bias voltage across the boundary, as shown by Fig. 5. A dramatic enhancement of CL intensity at applied voltages less than 2 V followed by the trend of the recovery to the initial CL value at higher voltages, in concordance with the prediction of the model B.

4. Conclusion

Dislocation network formed at the interface of directly bonded *p*-type silicon wafers accompanies with a high density of donor-like electronic states creating a high electrical barrier for the current flow across the boundary. Two deep level traps ($E_v + 0.3$ eV (DT1), $E_v + 0.4$ eV (DT2)) and one shallow trap $E_v + 0.08$ eV (DT3) were found by means of the capacitance transient spectroscopy technique. Two channels (models) of the excess carrier recombination via existing deep levels at the boundary were considered and their predictions of the character of the CL excitation level dependence and of the impact of the applied voltage are in agreement with the experimental obtained data. It was concluded that most of the excess carriers reaching the dislocations recombine nonradiatively via the deep electrical levels whereas the D1–D2 radiative recombination occurs via coupled transition between two shallow levels.

References

- [1] V. Kveder, M. Badylevich, E. Steinman, A. Izotov, M. Seibt, W. Schroter. *Appl. Phys. Lett.*, **84**, 2106 (2004).
- [2] T. Sekiguchi, S. Ito, A. Kanai. *Mater. Sci. Eng. B*, **91–92**, 244 (2002).
- [3] M. Kittler, M. Reiche, T. Arguirov, W. Seifert, X. Yu. *IEDM Tech. Digest*, **1027** (2005).
- [4] M. Kittler, T. Arguirov, W. Seifert, X. Yu, M. Reiche. *Sol. St. Phenomena*, **108–109**, 749 (2005).
- [5] X. Yu, O.F. Vyvenko, M. Reiche, M. Kittler. *E-MRS Spring Meeting 2006*, May 29–June 3, 2006, Nice, France.
- [6] M. Kittler, X. Yu, O.F. Vyvenko, M. Birkholz, W. Seifert, M. Reiche, T. Wilhelm, T. Arguirov, A. Wolff, W. Fritzsche, M. Seibt. *Mater. Sci. Eng. C*, **26** (5–7), 902 (2006).
- [7] F.M. Livingston, S. Messoloras, R.C. Newman, B.C. Pike, R.J. Stewart, M.J. Binns, W.P. Brown, J.G. Wilkes. *J. Physics C (Sol. St. Phys.)*, **17** (34), 6253 (1984).
- [8] A. Broniatowski. *Philosophical Magazine B (Physics of Condensed Matter, Electronic, Optical and Magnetic Properties)*, **66**, 767 (1992).
- [9] A.J. Kenyon, E.A. Steinman, C.W. Pitt, D.E. Hole, V.I. Vdovin. *J. Phys.: Condens. Matter*, **15**, 2843 (2003).
- [10] X. Yu, T. Arguirov, M. Kittler, W. Seifert, M. Ratzke, M. Reiche. *Mater. Sci. Semicond. Proc.*, **9**, 96 (2006).
- [11] E.A. Steinman. *Phys. Status Solidi C*, **2**, 1837 (2005).
- [12] V. Kveder, M. Badylevich, W. Schroter, M. Seibt, E. Steinman, A. Izotov. *Phys. Status Solidi A*, **202**, 901 (2005).

Редактор Л.В. Беляков